CIRP Annals - Manufacturing Technology 67 (2018) 79–82

Contents lists available at ScienceDirect

CIRP Annals - Manufacturing Technology

journal homepage: http://ees.elsevier.com/cirp/default.asp

Influence of oxygen on the tool wear in machining

Volodymyr Bushlya [a,*], Filip Lenrick [a], Jan-Eric Ståhl [a], Rachid M'Saoubi (1)[b]

[a] Division of Production and Materials Engineering, Lund University, Ole Römers väg 1, 22100, Lund, Sweden
[b] R&D Materials and Technology Development, Seco Tools AB, SE-73782, Fagersta, Sweden

ARTICLE INFO

Article history:
Available online 22 April 2018

Keywords:
Machining
Wear
Oxidation

ABSTRACT

High temperatures generated in machining are known to facilitate oxidation wear. A controlled atmosphere chamber was developed to investigate the effects of oxygen on tool wear and high speed machining tests were conducted on air and in argon. Cemented carbide, cermet and cubic boron nitride tooling was used on alloyed steel, hardened tool steel and superalloy Alloy 718. Machining in argon resulted in higher flank wear, higher cutting forces, and larger tool–chip contact length on the rake face. However, in hard machining, argon atmosphere reduced rake cratering. Transmission electron microscopy of tools worn on air showed formation of nanocrystalline Al_2O_3 film on the rake when machining aluminium containing Alloy 718, while no oxide films was detectable in the other cases.

1. Introduction

Oxidation in machining is one of the mechanisms – alongside with abrasion, adhesion, and diffusion – which govern tool deterioration [1].

Investigation of the oxygen impact on the machining process requires the use of oxygen-free environment, such as in a vacuum or inert gas chamber [1–9]. Majority of studies address the issues of machining mechanics: cutting forces [2,3], tool–chip contact length [4,5], friction [4,6], build-up edge formation [2], and surface quality [2]. It was shown that the impact of the oxygen-free environment is defined by the tool-workpiece material pair. Machining of iron [2,5] and copper [3] in vacuum demonstrate an increase of forces and contact length, while machining of aluminium [6] results in decreased or invariable force and contact parameters for carbon steel, HSS and coated tooling.

The impact on tool wear, however, was given less attention. It was shown that the reduction of O_2 content results in the decrease of notch wear for cemented carbide tools [7,10]. Similar impact of the oxygen-free environment was found on the tool rake cratering in turning cooper [9] and milling stainless steel [8].

In this study, oxidation wear mechanism in high speed machining with cemented carbide, cermet, pcBN tooling and different workpiece materials was investigated.

2. Experimental work

The developed controlled environment chamber represents a steel box with gas curtain tubing in the upper part (Fig. 1a). Another gas supply circuit represents 3 secondary nozzles attached above and on the sides of a toolholder. Gas is also introduced into the cutting zone through 3 primary nozzles of PDJNL3225P15JETL (Seco Tools) high pressure jet holder (Fig. 1a and b). The curtain and secondary nozzles are connected to one gas flow regulator, while the primary nozzles to another regulator. Frontal box opening was covered with a safety glass for visual observation of the machining process. The lower part of the chamber has an opening for chip evacuation.

ARCAL Prime gas supplied by Air Liquide with the purity of argon 99.998% and content of $O_2 \leq 5$ ppm was used in the tests. Initial machining tests with a flow rate of 35 l/min and gas pressure of 1.8 bar through each set of nozzles has shown insufficient protection of the tool rake and the flank, similarly to Ref. [7]. Increase of the flow per nozzle set to 100 l/min at 3.2 bar prevented oxidation on the tool rake, however oxide deposit on the flank remained in the direct vicinity of the wear land. Only one nozzle supplies argon directly towards the flank while five nozzles and the curtain protect the rake. Further increase to 200 l/min at 4.7 bar ensured approx. 250 μm band of oxide free region on the flank (Fig. 1d). Therefore a total of 400 l/min, or one complete exchange of atmosphere in the controlled environment chamber every 0.15 s, was maintained during the machining tests in Ar. After disengagement the gas flow was kept for another 180 s to exclude tool oxidation during cooling. Machining on air was done under identical conditions, but using filtered compressed air, in order to assert similar gas circulation and cooling. It was shown [5] that the oxygen partial pressure of ≤1 mbar or ≤0.1% was sufficient for oxidation prevention in machining ferrous alloys, and therefore current setup is referred to as oxygen-free environment throughout the paper.

Machining was done at two cutting speeds, while depth of cut and feed were selected to ensure proper chip breaking and

* Corresponding author.
E-mail address: rachid.msaoubi@secotools.com (R. M'Saoubi).

https://doi.org/10.1016/j.cirp.2018.03.011
0007-8506/

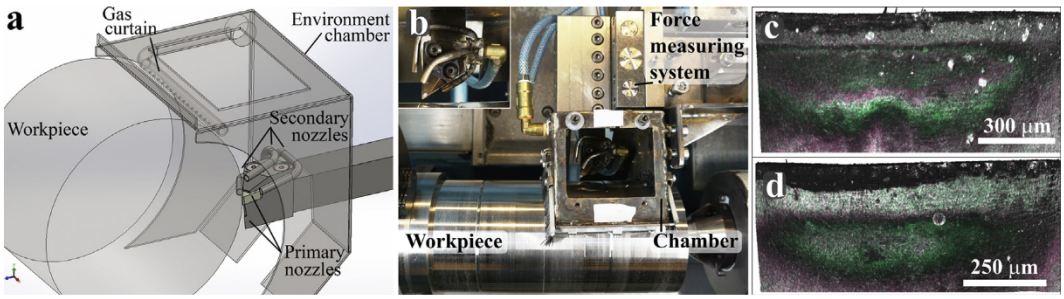

Fig. 1. (a) Schematic of the controlled environment chamber; (b) experimental setup when machining Alloy 718; oxide deposit on the flank of cemented carbide tool after 45 s machining (c) on air and (d) in argon.

Table 1
Experimental test array.

Tool material	Tool grade	Workpiece	v_c, m/min	f, mm/rev	a_p, mm	Gas
Cemented carbide	P10	34CrNiMo6	250, 280	0.35	1.00	Air, Ar
Cermet	210	34CrNiMo6	180, 200	0.30	1.00	Air, Ar
PCBN	CBN170	Alloy 718	300, 350	0.10	0.25	Air, Ar
PCBN	CBN010	Caldie	150, 200	0.05	0.25	Air, Ar

evacuation (Table 1). Wear of four tool material grades, including cemented carbide, cermet and pcBN, was investigated in machining alloyed steel, hardened cold work tool steel, and aged Alloy 718.

Optical microscopy and 3D reconstruction was performed on a Alicona InfiniteFocus. Scanning electron microscopy (SEM) was performed on a Tescan Mira3 equipped with field emission gun and Oxford EDX detector. Focus ion beam (FIB) lamella preparation was performed on a FEI Nova NanoLab 600 dual beam FIB/SEM. Standard *in-situ* lift-out procedure was employed where the lamellae were thinned to electron transparency (approx. 100 nm) using 10 kV Ga+ ions. Transmission electron microscopy (TEM) was performed on a JEOL 3000F equipped with field emission gun and Oxford EDX detector.

Uncoated P10 grade of cemented carbide was selected because it has been shown to have highest resistance to oxidation wear among the steel cutting grades [10]. Uncoated cermet with Ni–Co binder was also selected for its high resistance to oxidation [11]. CBN170 (Seco Tools) is a SiC whisker reinforced grade with 65 vol.% content of cBN and multi-modal grain size distribution specifically designed for machining superalloys. CBN010 (Seco Tools) is a signature grade with 50 vol.% content of cBN and TiC binder for finishing hard machining. All inserts were of ISO DNGA150608 type geometry. Cemented carbide and cermet have commercial chip-breakers. CBN010 has a chamfer with $b_\gamma = 0.1$ mm land and $\gamma_f = 20°$ angle. CBN170 has a flat rake.

3. Results and discussion

Fig. 2 shows the evolution of the cutting forces against flank wear (VB) for all machining cases. It can be seen that the influence of oxygen-free environment depends on the tool-workpiece material pair, as also reported in Ref. [3]. Strongest impact was found in machining with cemented carbide where argon environment resulted in an increase of F_c force by ≈15% and by ≈25% for feed F_f and passive F_p forces. In machining with cermet only the cutting force component F_c was increased by ≈10% (Fig. 2b). In machining Alloy 718 force data are inconclusive, because an additional mechanism of notching and premature edge failure (Fig. 7) dominates forces more than the environment.

Williams and Tabor [5] attributes the increase of forces in the oxygen-free environment to disappearance of slip zone and expansion of stick zone over the entire tool–chip contact, also observed in this study (Fig. 8c). This is also accompanied by larger contact length [2,3,5]. Application of commercial chip-breakers in our study creates restriction to a contact zone, thus limiting force increase only to stick zone effect.

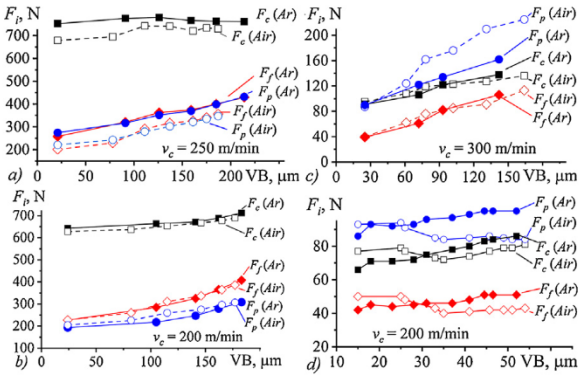

Fig. 2. Development of cutting forces with tool wear for (a) cemented carbide, (b) cermet, (c) CBN170, and (d) CBN010.

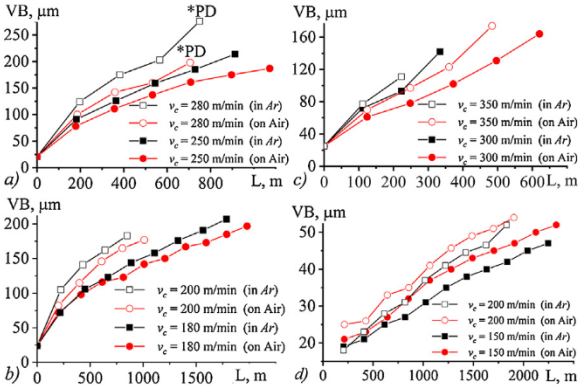

Fig. 3. Development of tool wear when machining on air and in argon by (a) cemented carbide, (b) cermet, (c) CBN170, and (d) CBN010. *PD stands for plastic deformation.

Fig. 3 shows the development of the flank wear land VB with the tool travel distance when machining on air and in argon. It can be seen that flank wear is more intensive in all cases when machining in argon, as compared to the air case. The same effect was consistently observed for both levels of cutting speed, implying that contribution of oxidation might be similar, as all tests are in the high-speed machining range.

Although the impact on rake face cratering was found to be pronounced when machining in oxygen-free environments [8,9], the impact on the flank wear has not been previously reported. In our cases of machining 34CrNiMo6 steel, cratering was suppressed by non-metallic inclusions in material microstructure, thus enabling to assess effects on flank wear.

The observed expansion of stick zone when machining in argon (Fig. 8c) is expected to aggravate secondary deformation in the flow zone [12]. This will lead to more intensive and localized heat source at the tool–chip interface [1]. Therefore an increased process temperature can be expected in these cases, thus explaining the observed intensification of flank wear when machining in oxygen-free environment. However, in the case of hard machining with CBN010, the contribution of oxidation wear

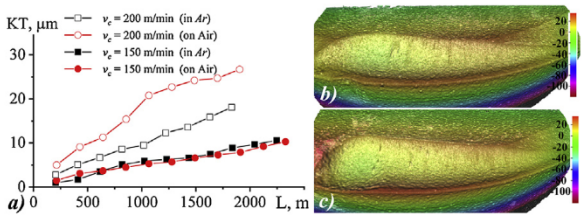

Fig. 4. (a) Development of crater wear when machining with CBN010, 3D view of CBN010 worn (b) in argon and (c) on air (v_c = 200 m/min).

mechanism outweighed (Figs. 3d and 4a) the other temperature-driven mechanisms such as diffusion and abrasion. Hard machining at lower cutting speed resulted in identical rake cratering, yet the crater wear was significantly intensified when machining on air at v_c = 200 m/min (Fig. 4a). This indicates that the oxidation mechanism was thermodynamically activated [13] at such high cutting speed (process temperature). Crater wear of $KT \geq 30$ μm lead to complete tool fracture.

Using optical microscopy, Trent and Wright [1] identified oxidized and non-oxidized regions on worn tools, where the oxide films were always found a distance away from the tool–chip–workpiece contact zone. The composition was interpreted from variations in colour and contrast. They assumed that adsorption of oxygen by the newly formed surfaces, also as found in Ref. [6], depleted the atmosphere around the edge, thus naturally creating oxygen-free pocket preventing near-edge oxidation. Also in our study, optical microscopy of worn cermet and carbide tools showed similar features. However, SEM BSE microscopy depicted a dark near-edge band which, combined with EDX mapping, demonstrate the formation of oxides over the entire clearance face (Fig. 5). EDX line scan along the clearance (Fig. 5b and c) shows: (i) higher O content, simultaneously with depletion of W, indicative of the formation of WO_3 [10] directly next to the cutting edge, and (ii) higher than background O levels and normal W further down are implying formation of TiO_2 film. Identical phenomena were found on the rake and in all other machining cases with carbide and cermet tooling. These findings prove, though oxygen adsorption does occur [6] it is insufficient to form an oxygen-free pocket that prevent oxidation.

Despite the observed intensification of flank wear when machining in oxygen-free environment (Fig. 3), its impact on the notch wear formation was found to be positive. Machining on air with carbide and cermet tooling was accompanied by notching on the major (Fig. 6a) and minor cutting edge. Yet, notching was completely blocked in argon environment (Fig. 6b). These findings are attributed to an easier abrasion of the above demonstrated WO_3 and TiO_2 oxides by the burrs [1].

However, a contrary influence on notching occurred in machining Alloy 718 with CBN170, where machining in argon resulted in significantly higher notch formation (Fig. 7). Adhesion and pluck-out of the tool material by the chips and burrs in machining Alloy 718 [14] was intensified in the absence of oxide film formation. Additionally, notching in argon expanded laterally,

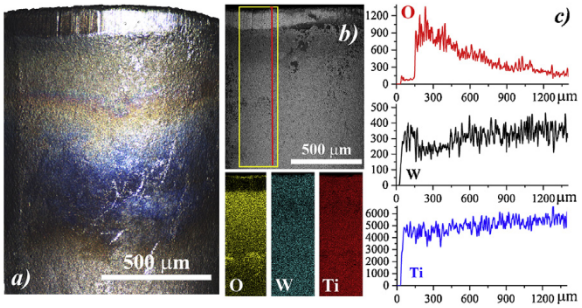

Fig. 5. (a) Optical and (b) BSE image of oxide deposit on cermet (v_c = 200 m/min) with EDX maps and respective line scan.

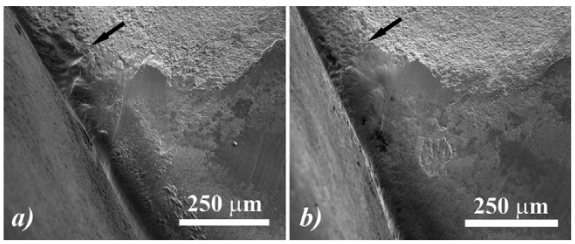

Fig. 6. Detailed SEM view of worn cermet rake when machining (a) on air, and (b) in argon (v_c = 200 m/min).

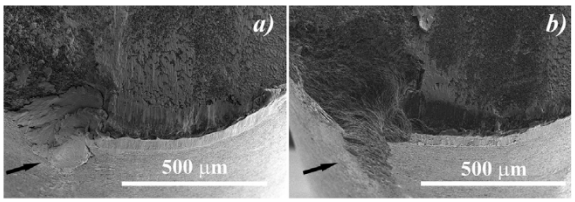

Fig. 7. SEM image of CBN170 tool after machining Alloy 718 (a) on air and (b) in argon environment (v_c = 350 m/min).

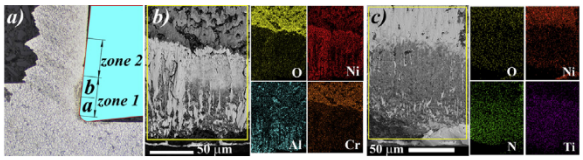

Fig. 8. (a) Schematic of contact zones (adapted from Ref. [4]). BSE image and EDX maps of CBN170 rake after machining Alloy 718 (b) on air and (c) in argon (v_c = 350 m/min).

leading to a gradual cutting edge deterioration and collapse (Fig. 7b).

Fig. 8b demonstrates the formation of a pronounced oxide layer formed outside the crater of CBN170 tool after machining on air. Fig. 8c illustrates the absence of such oxides, thus confirming oxygen-free environment when machining in argon. When machining on air, two contact zones are distinguished in the contact area (Fig. 8b), alongside with considerable workpiece material adhesion, as verified by EDX Ni element mapping. Additionally, presence of Al and O in the crater suggests the formation of Al_2O_3. Machining in argon (Fig. 8c) results in a single contact zone and suppression of material adhesion. Doyle et al. [4] demonstrated presence of stick (zone 1) and slip (zone 2) regions on the rake (Fig. 8a). Zone 2, in their study, was characterized by gross transfer of chip material onto the rake, as also seen in Ref. [15] and in our study. They attribute this mechanism to the formation of oxide films in this region and higher friction coefficient in the presence of oxides. Thus it can be concluded that oxygen-free environment promotes stick region (zone 1).

Fig. 9 shows scanning (S)TEM dark field (HAADF) images from thin cross sections of CBN170 and CBN010 tool rake surfaces prepared by FIB after machining on air. In both cases, preferential removal of cBN phase is observed, as seen by the position of interface line between the adhered metal and tool material. The mechanism is believed to be diffusional, where elemental boron and nitrogen are dissolved in the chips. The metal–cBN interface moves faster than the binder, which is then abraded [16], and eventually the entire cBN grain is consumed and replaced by a metal. However, this phenomenon is more pronounced when hard machining Caldie tool steel (Fig. 9b), as compared to machining Alloy 718 (Fig. 9a).

SEM and associated EDX data did not reveal the presence of oxide films directly on the tool–chip or tool–workpiece interfaces, which is expected due to limitations of thin film detection for this technique. Therefore, FIB prepared cross section lamellae were investigated with TEM. As can be seen in Fig. 10a a layer of iron

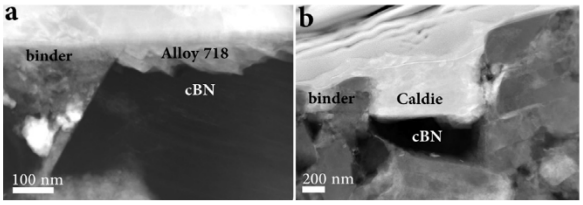

Fig. 9. STEM HAADF image of lamellae extracted from the crater of (a) CBN170 (v_c = 300 m/min) and (b) CBN010 (v_c = 150 m/min) after machining Alloy 718 and Caldie on air.

oxide is located atop a grain of TiC, yet no TiO_2 was found. The adhered film of Fe is believed to have oxidised upon cooling after tool disengagement. Oxide was not found in the sample of CBN010 when hard machining on air (Fig. 10b) either. Despite the absence of oxides when inspecting the samples with SEM and TEM, the mechanism of oxidation wear cannot be ruled out. The expected

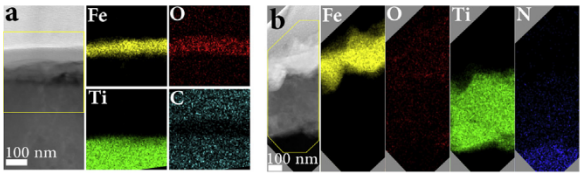

Fig. 10. STEM HAADF image with EDX maps of lamellae from (a) flank of cemented carbide and (b) crater of CBN010 after machining on air.

oxides, WO_3, TiO_2 and B_2O_3, either lack mechanical or chemical stability and are easily removed during machining.

Fortunately after machining Alloy 718 on air, an oxidation process on the tool–chip interface was detectable since Alloy 718 contains Al (and Ti) which gives rise to the mechanically and chemically stable Al_2O_3 (Fig. 11a). Judging from this observation, oxidation most likely occurs in all other cases when machining on air, as the mechanics of high-speed machining are very similar. For the test performed in argon (Fig. 11b), a film of Al is also seen, but as the oxygen signal is a pure noise without correlation to the Al signal, Al_2O_3 is ruled out. Since TiN was found on the tool–chip interface, due to a reaction of Ti and cBN, a formation of a (Ti,Al)N film seems likely. Verifying this hypothesis would however require additional investigation.

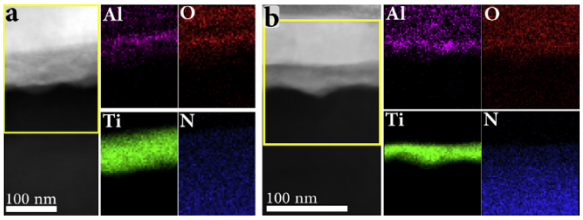

Fig. 11. STEM HAADF image with respective EDX maps of lamellae from CBN170 after machining Alloy 718 (a) on air and (b) in argon.

Presence of Al_2O_3 and TiN atop a cBN grains creates a diffusional barrier, which retards diffusional wear of cBN. This explains the difference in cBN wear rate when hard machining Caldie (Fig. 9), which does not contain elements capable of forming such barriers.

4. Conclusions

Oxidation wear mechanism in high speed machining with cemented carbide, cermet and pcBN tooling was investigated. The results indicate that the impact of oxygen-free environment on the cutting forces varies for different tool-workpiece pairs. Flank wear was found to be more intensive when machining in argon, except for the case of hard machining with pcBN. In this case, cratering was found to be more intensive in oxidative atmosphere. However, the oxidation mechanism was activated only at high cutting speed. In contrast, cratering was reduced in machining Alloy 718 due to oxidation of workpiece material and formation of a deposit of Al_2O_3 on the tool. Concurrently, reaction of the workpiece and cBN resulted in TiN deposit, both of which acted as diffusion barrier.

Acknowledgements

This research was supported by European Union's Horizon 2020 Research and Innovation Programme under Flintstone 2020 project (grant agreement No. 689279). The authors also would like to express their gratitude to Mikael Hörndahl for the help with chamber build-up.

References

[1] Trent EM, Wright PK (2000) *Metal Cutting*, 4th ed. Butterworth-Heinemann, Oxford.
[2] Rowe GW, Smart EF (1963) The Importance of Oxygen in Dry Machining of Metal on a Lathe. *British Journal of Applied Physics* 14:924–926.
[3] Doyle ED, Horne JG (1980) Adhesion in Metal Cutting: Anomalies Associated with Oxygen. *Wear* 60:383–391.
[4] Doyle ED, Horne JG, Tabor D (1979) Frictional Interaction Between Chip and Rake Face in Continuous Chip Formation. *Proceedings of the Royal Society of London Series A* 366:173–183.
[5] Williams JA, Tabor D (1977) The Role of Lubricants in Machining. *Wear* 43:275–292.
[6] Wakabayashi T, Suda S, Inasaki I, Teresaka K, Musha Y, Toda Y (2007) Tribological Action and Cutting Performance of MQL Media in Machining Aluminum. *Annals of the CIRP* 56:97–100.
[7] Tennenhouse GJ, Runkle FD (1987) The Effects of Oxygen on the Wear of Tungsten-Carbide-Based Materials. *Wear* 118:365–375.
[8] Yamane Y, Narutaki N (1983) The Effects of the Atmosphere on Tool Failure in Face Milling (1st Report). *Journal of Japanese Society for Precision Engineering* 49:521–527.
[9] Shimada S, Inamura T, Higuchi M, Tanaka H, Ikawa N (2000) Suppression of Tool Wear in Diamond Turning of Copper Under Reduced Oxygen Atmosphere. *Annals of the CIRP* 49:21–24.
[10] Tuininga EJ (1967) Wear and Oxidation Phenomena on the End Cutting Edge of Carbide Turning Tools. *Annals of the CIRP* XIV:449–463.
[11] Akasawa T, Takeshita H, Uehara K (1987) Hot Machining With Cooled Cutting Tools. *Annals of the CIRP* 36:37–40.
[12] Jawahir IS, van Luttervelt CA (1993) Recent Developments in Chip Control Research and Applications. *CIRP Annals— Manufacturing Technology* 42:659–693.
[13] Klimenko SA, Polonskij LG, Murovoz YuA (1993) Influence of Gaseous Mediums on Kiborit Tool Wear When Used to Turn Coatings. *Sverkhtverdye Materialy* 4:35–39.
[14] Bushlya V, Zhou J, Avdovic P, Ståhl J-E (2013) Wear Mechanisms of Silicon Carbide-Whisker-Reinforced Alumina (Al_2O_3-SiC_w) Cutting Tools When High-Speed Machining Aged Alloy 718. *International Journal of Advanced Manufacturing Technology* 68(5–8):1083–1093.
[15] M'Saoubi R, Chandrasekaran H (2005) Innovative Methods for the Investigation of Tool-chip Adhesion and Layer Formation During Machining. *CIRP Annals—Manufacturing Technology* 54:59–62.
[16] M'Saoubi R, Johansson MP, Andersson JM (2013) Wear Mechanisms of PVD-Coated PCBN Cutting Tools. *Wear* 302:1219–1229.